Journal of Materials Processing Technology 211 (2011) 1678–1683

Contents lists available at ScienceDirect

Journal of Materials Processing Technology

journal homepage: www.elsevier.com/locate/jmatprotec

Laser-guided discharge texturing for cold mill roller

Wang Zhitong*, Yang Mingjiang

Institute of Mechanics, Chinese Academy of Sciences, Beijing 100190, China

ARTICLE INFO

Article history:
Received 1 August 2010
Received in revised form 29 April 2011
Accepted 10 May 2011
Available online 14 May 2011

Keywords:
Surface texturing
Laser-guided discharge Texturing
Surface topography
Arc pressure

ABSTRACT

This paper presents a new method of surface texturing for the cold mill roller called laser-guided discharge texturing to acquire the high surface roughness. In this method, the pulsed laser was focused on the roller surface to produce the metal plasma, and was then used to guide the arc discharge in the gap of electrodes to texture the roller. Laser-guided discharge texturing absorb the advantages of electrical discharge texturing and YAG laser texturing to form the following properties: the quick processing speed, the high processing energy, the deterministic distribution of the textured craters, and the enhanced surface shaping to the textured craters. In this paper, the control of the laser guiding in the randomicity of the discharge craters was studied, the surface topography of the textured craters was studied with different current peaks and pulse-widths, and the microstructures of the textured craters were analyzed.

1. Introduction

Now, the technology of the roller surface texturing has widely been applied in the cold rolling industry. The surface texturing for the roller may increase the frictional coefficient between the roller and the steel sheet so as to decrease the surface defects of the steel sheet. On the other hand, the convex rims on the surface of the textured roller were converted to the concave pits on the surface of the steel sheet in the cold rolling process. The concave pits on the surface of the steel sheet may improve the performances of stamping and painting; therefore, the cold rolled textured sheets had widely been used in the body of the car. Now common methods of roller surface texturing include, a shot blast texturing (SBT), an electrical discharge texturing (EDT), a laser texturing (LT), and an electron beam texturing (EBT). The laser texturing can be further divided into two types: a CO_2 laser texturing (CO_2LT) and a YAG laser texturing (YAGLT). Simão et al. (2002) researched to alloy the roller surface using the powder metallurgy electrodes and sintered electrodes in the process of EDT. Surface roughness assessments showed that the topographical characteristics of alloyed EDT samples to be similar to those of conventional EDT samples, but the hardness of the alloyed EDT samples was higher. Elkoca (2008) studied the properties of the recast white layer on the surface of the skin pass mill work roll by EDT. It was found that the electrical discharge texturing led to a dramatic hardness drop in the white layer and the heat-affected zone, which was attributed to the high amount of retained austenite. Additionally, de-ionised water was found to be a promising dielectric liquid to abstain from retained austenite. Mingjiang (1998) researched the YAGLT method by the quasi-continuous Nd:YAG laser. The characteristics of this technology were compared with those of the CO_2LT, and the application of this technology in the industry was introduced. Du et al. (2005) studied the YAGLT method by pulsed Nd:YAG laser. The relationship between the laser processing parameters and the surface topography of the textured crater was studied. Gorbunov et al. (2009) compared five surface texturing methods for working rollers including: SBT, EDT, CO_2LT, YALT and EBT. These methods are used to ensure standard surface topography in the production of auto-industry sheet. The advantages and disadvantages of each method are outlined.

The distribution and the shape of the textured craters on the surface of the textured steel sheet by EDT all is random; therefore, in the stamping process the lubricating oil between the steel sheet and the mould will flow along the channels between the textured craters to weaken the lubricating condition. But the processing speed of EDT is fastest among the existing texturing methods except the traditional SBT; therefore, EDT has been widely applied in the cold rolling industry. On the contrary, the distribution of the textured craters on the surface of the textured steel sheets by YAGLT is deterministic, and the shape of those is separated so as to store easily the lubricating oil to improve the lubricating condition between the steel sheet and the mould; therefore, the stamping performance of the textured steel sheet by YAGLT is perfect. But the Q-switcher power in the YAG laser machine is limited; therefore, the processing speed and the surface roughness were not increased at same time to restrict the application of YAGLT technology in the cold rolling industry. It is obviously that a new kind of surface texturing method need to absorb the advantages of the laser processing and

* Corresponding author. Tel.: +86 010 82544260; fax: +86 010 82544261.
E-mail address: ztwang@imech.ac.cn (W. Zhitong).

0924-0136/$ – see front matter © 2011 Elsevier B.V. All rights reserved.
doi:10.1016/j.jmatprotec.2011.05.008

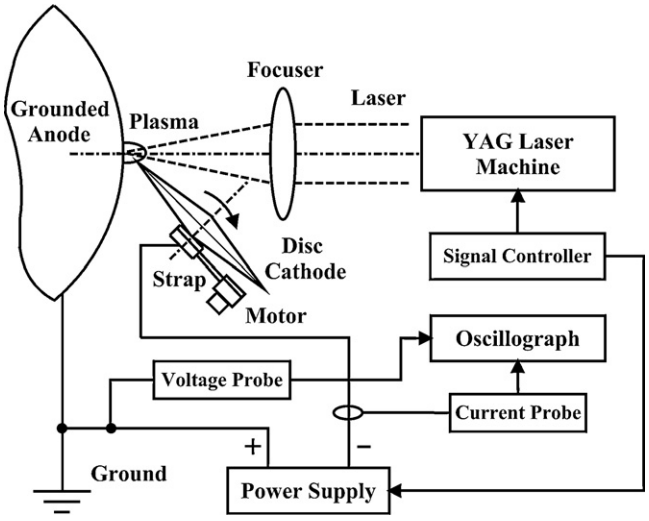

Fig. 1. Schematic of LGDT.

the electrical discharge processing. Zhitong et al. (2009) studied a method of surface strengthening to 1045 steel by laser guiding discharge, and compared the properties of the strengthened area by laser guiding discharge with those by the conventional discharge. Recently, Zhitong et al. (2010) experimentalized the control of the Laser guiding in the randomicity of the arc discharge. In this paper, EDT and YAGLT was integrated into together to form a new method of the surface texturing for the roller, called laser-guided discharge texturing (LGDT), inclined to process the high surface roughness on the surface of the cold mill roller.

In the method of LGDT, the pulsed laser was focused on the roller surface to produce metal plasma, and was then used to guide the arc discharge in the gap of electrodes to texture the roller surface. LDGT absorb the advantages of EDT and YAGLT in order to (1) utilize the high modulated frequency of quasi-continuous YAG laser to supply the high processing speed and the big arc discharge energy to produce the high surface roughness on the surface of the roller, and (2) control the randomicity of the arc discharge by laser guiding to design the distribution and the surface topography of the textured craters as well as to enhance the arc pressure to shape the surface of the textured craters.

This paper is divided into two sections. The first section presents the principle experiment of LGDT. The control of the laser guiding in the randomicity of the discharge craters is studied. The second section presents the processing experiment of LGDT. The surface topography of the textured craters is studied with different processing parameters, and the microstructures of the textured craters are also analyzed.

2. Experimental equipment and methods

The experimental schematic is shown in Fig. 1, and the photo of the actual experimental equipment is shown in Fig. 2. A roller with a diameter of 60 mm and made of 1045 steel was considered as an anode and grounded. A 160-mm round disk made of copper was used as a cathode. The disk edge had a radius of about 0.3 mm. In the processing of LGDT, the roller was rotated on the lathe, while the disk was also rotated and moved along the axis of the roller. Using the rotated disk, the sequential discharge position on the disk edge was separated to improve the cooling condition; therefore, the disk life and the processing stability were increased. The rotational speed of the roller and the moving speed of the disk were controlled together to design the distribution of the textured craters.

Fig. 2. Photo of actual LGDT equipment.

YAG laser was used to guide the arc discharge with the following parameters: 10 mJ pulse energy, 120 ns pulse-width, and 1.06 μm wavelength. The diameter of the laser focus was approximately 0.4 mm, and the gap between the electrodes was 0.4 mm. The laser pulse and the discharge pulse were triggered synchronously through the controlling signal. The transformer oil was initially applied on the roller surface to restrict the expansion of the textured craters. The thickness of the oil film was approximately 0.1 mm. The waveforms of the discharge voltage and the discharge current are shown in Fig. 3.

The main subject of this paper consists of the surface topography of textured craters as a result of laser-guided discharge. Surface 3D Profiling Micro-XAM was used to measure the three-dimensional (3D) topography of the textured craters. The height of the convex rims and the depth of the concave pits of the textured craters were measured. Afterwards, the 3D surface roughness SRa based on plane measurement was also computed.

The surface photos of the textured craters were taken using 3D microscope Stemi SV11. The diameter of the textured craters was measured. The cross-section samples of the textured craters were prepared, after which their microstructures were analyzed. The hardness of the textured craters was also measured.

3. Principle experiment of LGDT

In order to study how the laser guiding to control in the randomicity of the discharge craters during the processing of arc discharge, the textured surface by laser guiding was compared with

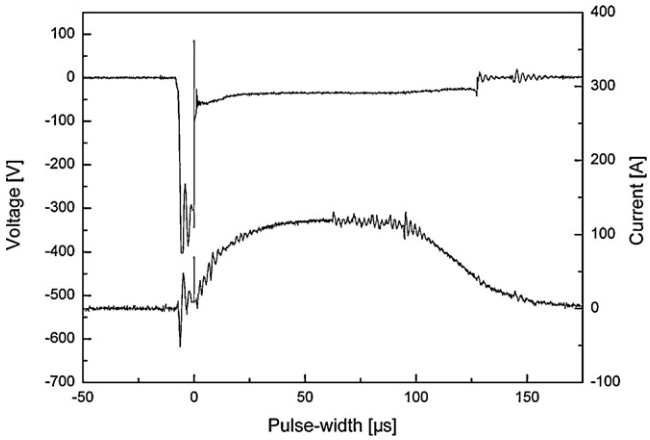

Fig. 3. Waveforms of current and voltage by LGDT.

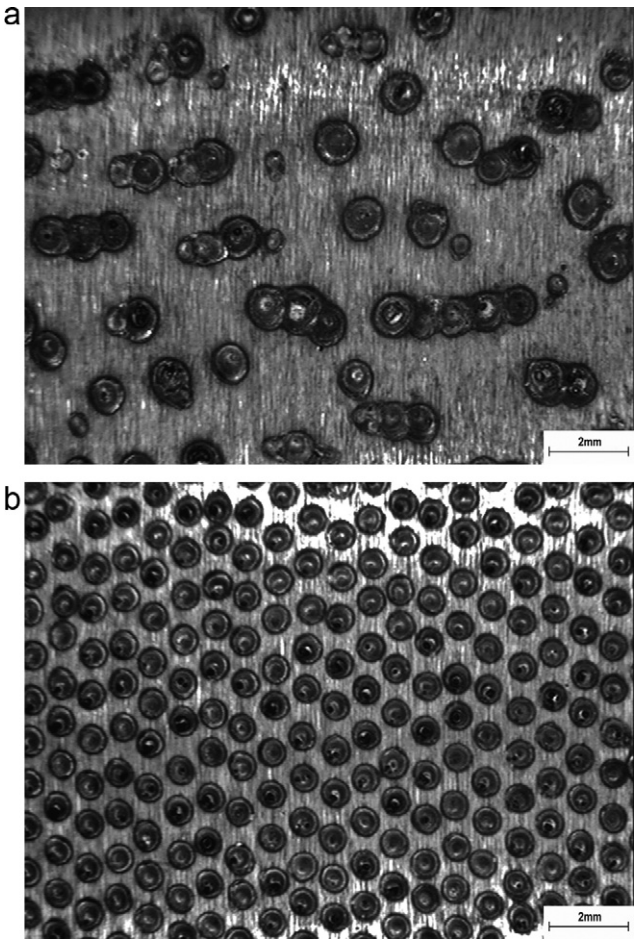

Fig. 4. Surface 3D microscope photos of textured surfaces by (a) common arc discharge, and (b) laser-guided discharge.

that by common arc discharge. In this study, the discharge voltage was maintained at 3000 V. The experimental result (Fig. 4) showed that without laser guiding, the distribution of the textured craters is random, the diameter of the textured craters is irregular, and some discharge pulses were not successfully triggered; but with laser guiding, the characteristics of the textured craters all is on the contrary.

The control schematic by laser guiding in the common arc discharge is shown in Fig. 5. Without laser guiding, the discharge position was determined by the microtopography of the electrode tip. The arc discharge spread along the path of the least energy, and the discharge position was random. With laser guiding, the laser pulse was focused on the material surface to produce the plasma. The arc discharge spread along the plasma path to make the discharge position overlap with the laser focus. In addition, the jitter of the discharge pulse-width was reduced to make the diameter of the textured craters regular.

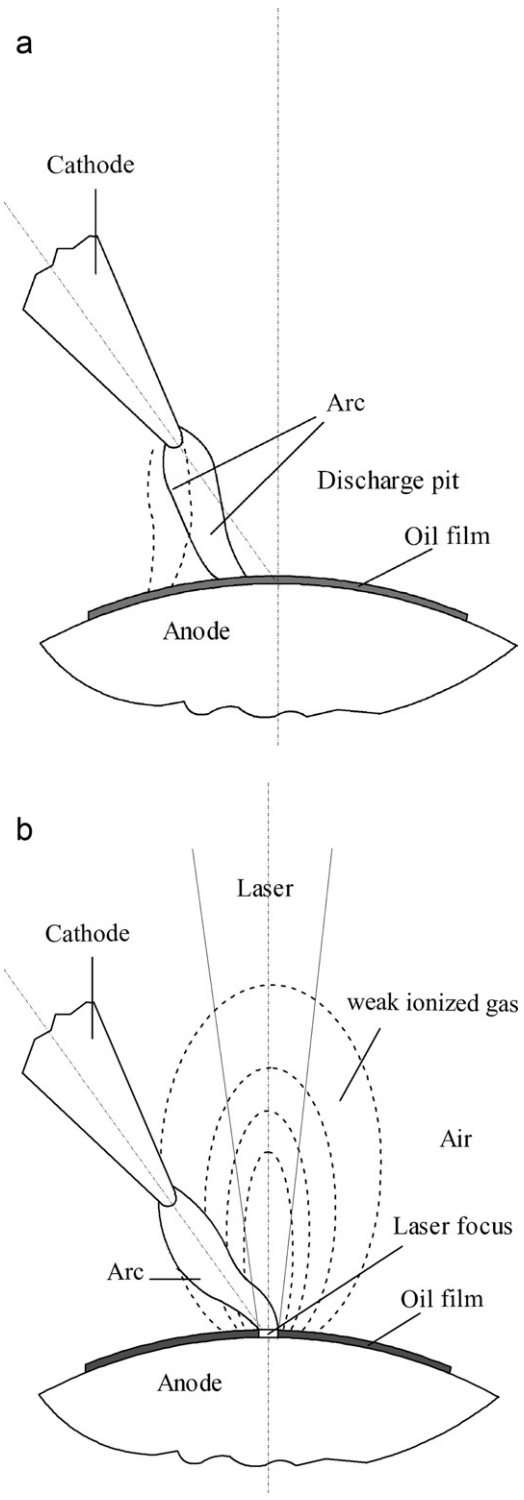

Fig. 5. Control schematic by (b) laser guiding in the (a) common arc discharge.

4. Processing experiment of LGDT

4.1. Surface topography of the textured craters with different current peaks

The processing parameters and experimental results are shown in Table 1. The arranged matrix of the textured craters was 0.66 mm × 0.78 mm. Surface 3D profile of the textured surfaces is shown in Fig. 6. The augment in the current peak increased the discharge energy, as a result, the diameter of the textured craters

Table 1
Experimental parameters and results.

Pulse-width (μs)	100			
Discharge current (A)	130	150	170	190
Pulsed discharge energy (J)	0.445	0.524	0.608	0.698
Diameter of textured crater (mm)	0.555	0.587	0.621	0.65
SRa of textured surface (μm)	6.03	6.26	7.53	8.46
Ratio of arc pressure	1	1.15	1.26	1.57

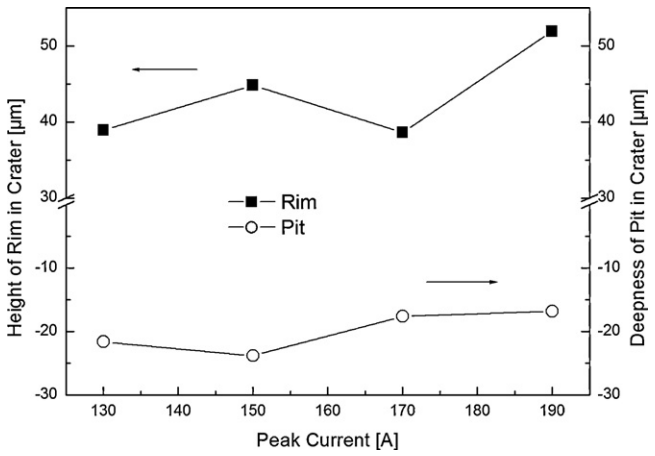

Fig. 6. Height of the convex rims and the depth of the concave pits in the textured craters with different currents.

was increased (Table 1). Huanzhong (1988) presented the arc pressure formula in the book. The arc pressure in accordance with the discharge current and the current density is presented as:

$$P_a \propto I \cdot j,$$

where P_a is the arc pressure, I is the discharge current, and j is the current density. Because the discharge energy and the arc pressure increased simultaneously with the augment in the current peak and the constant pulse-width, the height of the convex rims in the textured craters was increased from 38.9 to 51.9 μm, and the depth of the concave pits appreciably deceased (Fig. 6). But the augment of the arc pressure changed the shape of the convex rims in the textured craters from smooth to sharp (Fig. 7).

4.2. Surface topography of the textured craters with different pulse-widths

The processing parameters and experimental results are shown in Table 2. The arranged matrix of the textured craters was the same with that stated in Section 4.1. With the augment in the pulse-width and the constant current peak, the discharge energy was increased, but the arc pressure was decreased; therefore, although the height

Table 2
Experimental parameters and results.

Current peak (A)	150			
Pulse-width (μs)	80	130	180	230
Pulsed discharge energy (J)	0.273	0.513	0.744	1.1
Diameter of textured crater (mm)	0.463	0.561	0.647	0.713
SRa of textured surface (μm)	3.27	6.01	9.25	13.2
Ratio of arc pressure	1.91	1.3	0.98	0.8

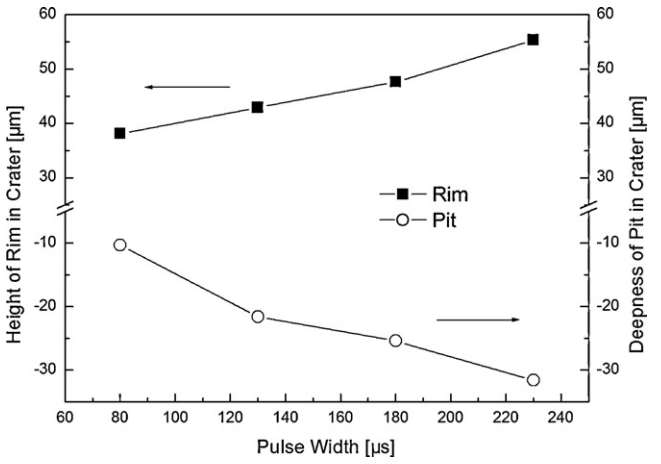

Fig. 8. Height of the convex rims and the depth of the concave pits in the textured craters with different pulse-widths.

of the convex rims in the textured craters was increased from 38.1 to 55.3 μm and the depth of the concave pits of the textured craters increased (Fig. 8), the shape of the convex rims in the textured craters changed from sharp to smooth (Fig. 9).

4.3. Microstructures of the textured craters

The optical microscope photo of a cross-section of a textured crater with 150 A current peak and 230 μs pulse-width is shown in Fig. 10. As can be seen, the microstructures of the textured crater can be divided into two sections: the melted section near the surface and the solid-state phase transition section near the base material. The hardness of the microstructures of the textured crater

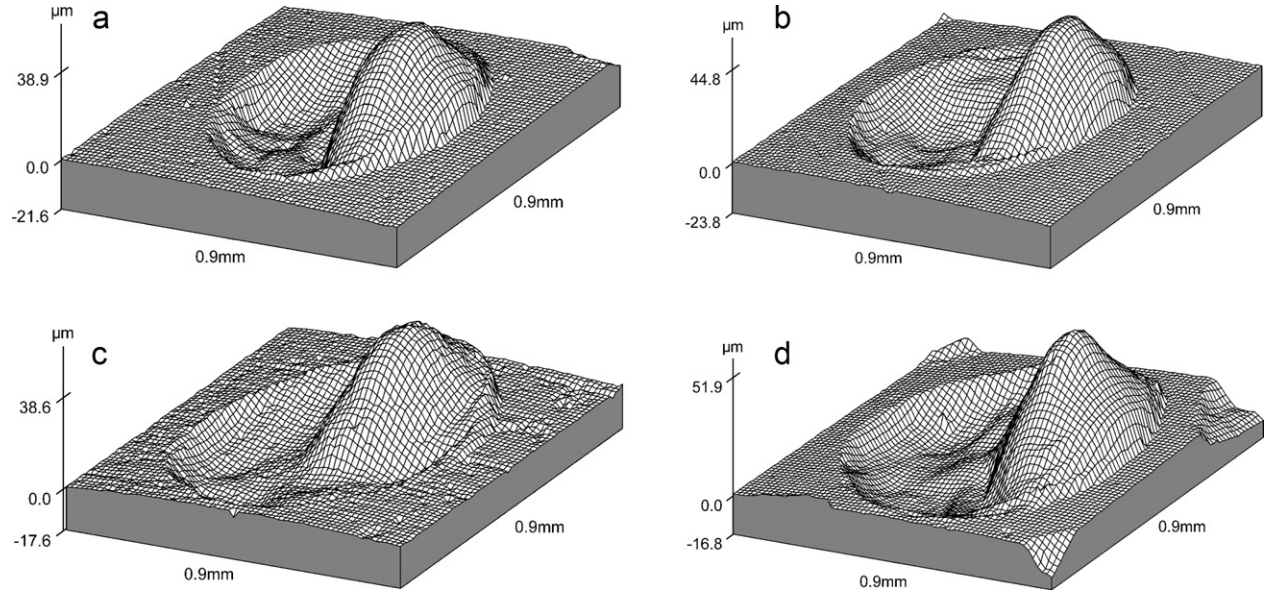

Fig. 7. Surface 3D profile of the textured craters with different currents: (a) 130 A, (b) 150 A, (c) 170 A, and (d) 190 A.

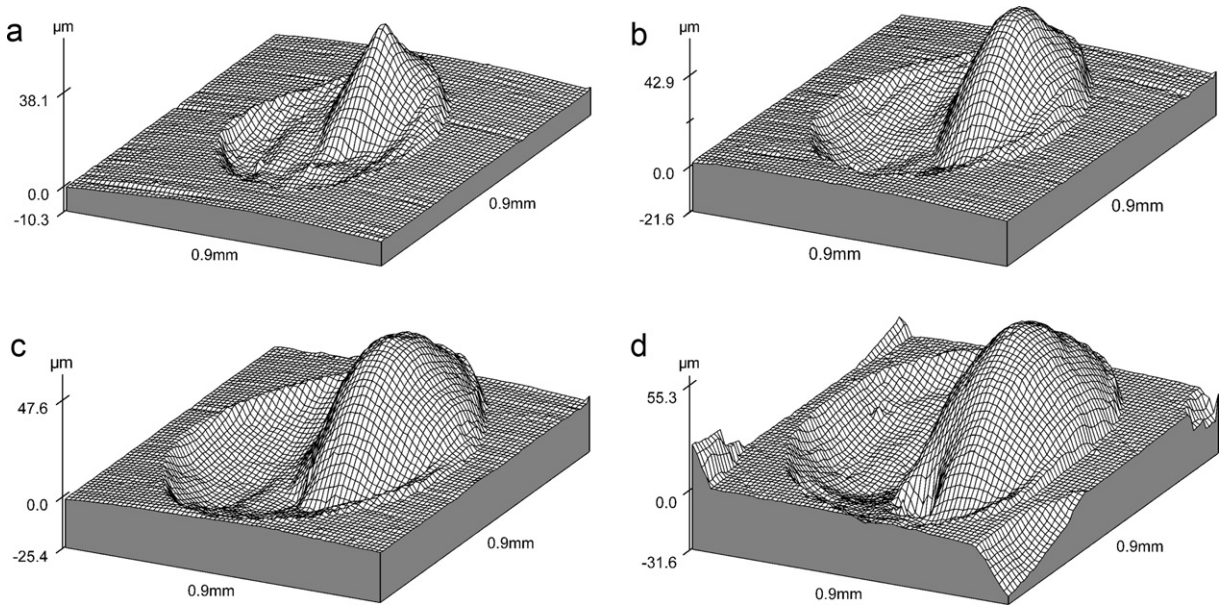

Fig. 9. Surface 3D profile of the textured craters with different pulse-widths: (a) 80 μs, (b) 130 μs, (c) 180 μs, and (d) 230 μs.

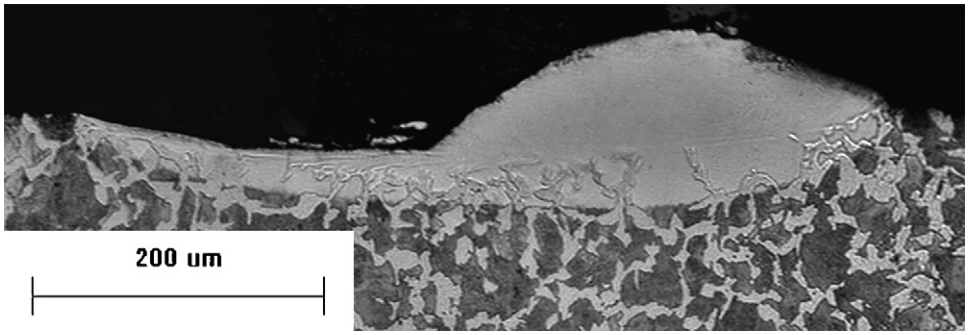

Fig. 10. Optical microscope photo of a cross-section of a textured crater with a current peak of 150 A and a pulse-width of 230 μs.

was measured. The measuring position started with the highest convex peak of the textured crater and ended at the base material. The hardness of six textured craters in Fig. 11 is from 800 to 1100 HV, about 2.7–3.7 times than that of the base material. With the augment of the current peak and the constant discharge pulse-width, the hardness of the textured craters was increased. But with the augment of the pulse-width and the constant current peak, the hardness of the textured craters was decreased. The hardness of the textured craters with short pulse-width and high current peak is higher than that with the other parameters.

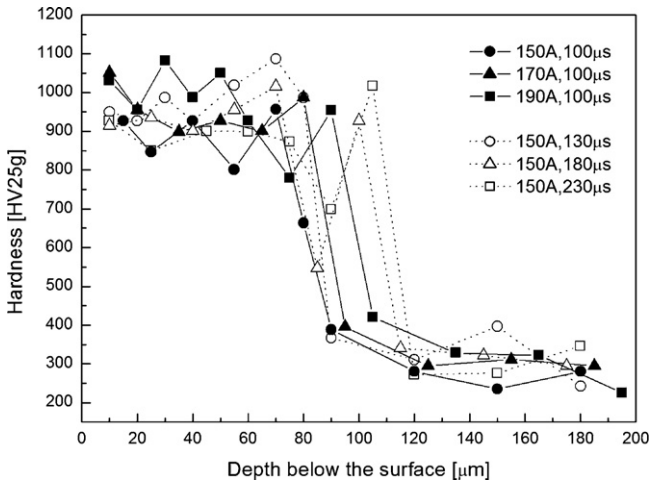

Fig. 11. Hardness of the textured craters with different discharge parameters.

5. Discussion

In order to compare the properties of three kinds of the textured craters by LGDT, YAGLT, and EDT, the surface topography of the textured crater by YAGLT and EDT need to be analyzed. The surface 3D profile of the textured craters by YAGLT was shown in Fig. 12. The diameter of textured crater by YAGLT is about 150 μm, and the height of the convex rims and the depth of the concave pits of the textured craters all are about 10 μm. The convex rims of laser-textured craters are ringy with many burrs. In the work by Simão et al. (2002), the roll surface by EDT with many burs is not clearly distinguished the textured craters. The height of the burs is about 11.5–34 μm. It is obviously that the textured craters by LGDT have combined the advantages of that by YAGLT and that by EDT to have the properties of the separated deterministic distribution, the highest convex rim, and the more smooth and regular shape of the convex rim.

The hardness and the shape of the convex rims in the textured craters determine the performance and the life of the textured roller surface together. The hardness of the textured craters is mainly determined by the cooling speed of the melted metal, which

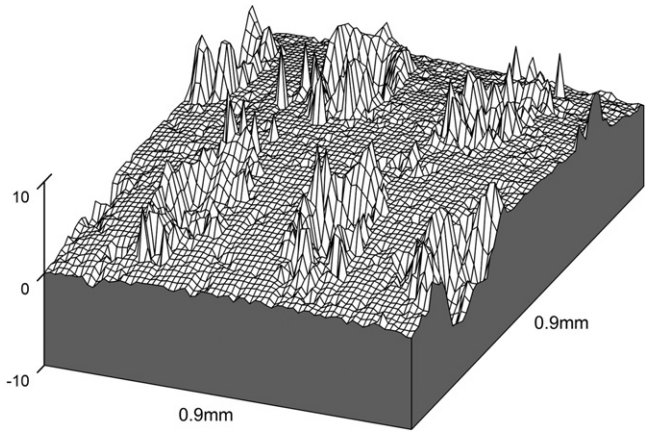

Fig. 12. Surface 3D profile of the laser-textured craters.

is controlled by two sides including the heat exchange between the melted metal and the air, and that between the melted metal and the base material. With the augment of the height of the convex rims in the textured crater the border area between the melted metal and the air was increased to quicken the heat exchange between the melted metal and the air; therefore, the hardness of the textured crater was increased. On the contrary, with the augment of the discharge pulse-width the heat exchange between the melted metal and the base material slower to decrease the hardness of the textured crater. In comparison of the hardness between the textured crater in Fig. 7d and that in Fig. 9d, it was found that although the border area between the latter and the air is even bigger than that between the former and the air, the hardness of the latter is still less than that of the former. Therefore, it is reasonable that the hardness of the textured crater is mainly determined by the heat exchange between the melted metal and the base material, and namely the discharge pulse-width. The shape of the convex rims in the textured craters is expected smooth. The arc pressure determined the shape of the convex rims in the textured craters. The high arc pressure produced the sharp convex rims in the textured craters; on the contrary, the low arc pressure produced the smooth convex rims in the textured craters. The height of the convex rims in the textured craters was mainly determined by the discharge energy, and the height of the convex rims in the textured craters increased with the augment in the discharge energy. Obviously, the parameters of a short discharge pulse-width and a low discharge current peak may supply the textured crater with a small diameter, a low height and a smooth shape of the convex rim adapted to produce the low roughness textured surface. The parameters of a long discharge pulse-width and a high discharge current peak may supply the textured crater with a big diameter, a high height and a smooth shape of the convex rim adapted to produce the high roughness textured surface.

6. Conclusion

The LGDT method was investigated in this paper, and the following conclusions were obtained from this study:

(a) The textured craters by LGDT have combined the advantages of that by YAGLT and that by EDT to have the properties of the separated deterministic distribution, the highest convex rim, and the more smooth and regular shape of the convex rim.
(b) The arc pressure increased with the augment in the current peak; thus, when the current peak increased from 130 to 190 A, the height of the convex rims in the textured craters increased from 38.9 to 48.7 μm, and the depth of the concave pits slightly decreased.
(c) The arc pressure decreased with the augment in the discharge pulse-width; but the augment in the discharge energy still increased the height of the convex rims in the textured craters from 38.1 to 55.3 μm, and the depth of the concave pits also increased.
(d) The hardness of the textured crater was about from 800 to 1100 HV, about 2.7–3.7 times than that of the base material. The hardness of the textured craters is determined by two sides including the height of the convex rims in the textured crater and the discharge pulse-width. With the augment of the height of the convex rims in the textured crater and the constant pulse-width, the hardness of the textured craters was increased. With the augment of the discharge pulse-width the hardness of the textured craters is always decreased regardless of the height of the convex rims in the textured crater. The hardness of the textured craters with short pulse-width and high current peak is higher than that with the other parameters.
(e) The parameters of the short discharge pulse-width and the low discharge current peak may supply some textured craters with a small diameter, a low height and a smooth shape of convex rims adapted to produce the low roughness textured surface. The parameters of a long discharge pulse-width and a high discharge current peak may supply some textured craters with a big diameter, a high height and a smooth shape of convex rims adapted to produce the high roughness textured surface.

Acknowledgements

The author is grateful for the support provided by the National Natural Science Fund of China (60877064). The author also wishes to extend his gratitude for the guidance of Dr. Yang Mingjiang, the Chief of the National Center for Laser-texturing Technology Development and Application.

Appendix A. Supplementary data

Supplementary data associated with this article can be found, in the online version, at doi:10.1016/j.jmatprotec.2011.05.008.

References

Du, D., He, Y.F., Sui, B., Xiong, L.J., Zhang, H., 2005. Laser texturing of rollers by pulsed Nd:YAG laser. J. Mater. Process. Technol. 161, 456–461.
Elkoca, O., 2008. A study on the characteristics of electrical discharge textured skin pass mill work roll. Surf. Coat. Technol. 202, 2765–2774.
Gorbunov, A.V., Belov, V.K., Begletsov, D.O., 2009. Texturing of rollers for the production of auto-industry sheet. Steel Transl. 39, 696–699.
Huanzhong, J., 1988. Arc Welding & Electro-slag Welding, 2nd ed. China Machine Press, Beijing, pp. 31–37.
Mingjiang, Y., 1998. Technology and Application of YAG Laser Texturing Cold-roll. In: Zhenzhong, G. (Ed.), Manual of Laser Processing. China Metrology Publishing House, Beijing, pp. 338–346.
Simão, J., Aspinwall, D., El-Menshawy, F., Meadows, K., 2002. Surface alloying using PM composite electrode materials when electrical discharge texturing hardened AISI D2. J. Mater. Process. Technol. 127, 211–216.
Zhitong, W., Mingjiang, Y., Mao, S., Yanliang, H., 2009. Surface strengthening of 45 steel by laser-guided micro discharge. Chin. J. Lasers 36, 2178–2181.
Zhitong, W., Zhongqiang, Z., Yanliang, H., Mao, S., Mingjiang, Y., 2010. Laser guiding in the randomicity of discrete surface strengthening by arc discharge. IEEE Trans. Plasma Sci. 38, 943–947.